Published in final edited form as:
Mol Cell. 2011 July 22; 43(2): 180–191. doi:10.1016/j.molcel.2011.06.017.

NF-κB Induction of the SUMO Protease SENP2: A Negative Feedback Loop to Attenuate Cell Survival Response to Genotoxic Stress

Moon Hee Lee[1], **Angela M. Mabb**[2], **Grace B. Gill**[3], **Edward T. Yeh**[4], and **Shigeki Miyamoto**[1,5]

[1]McArdle Laboratory for Cancer Research, Department of Oncology, University of Wisconsin-Madison, 6159 Wisconsin Institute for Medical Research, 1111 Highland Avenue, Madison, WI 53705, USA

[2]Department of Cell and Molecular Physiology, University of North Carolina, Chapel Hill, NC 27599, USA

[3]Department of Anatomy and Cellular Biology, Tufts University School of Medicine, Boston, MA, USA

[4]Department of Cardiology, University of Texas M. D. Anderson Cancer Center, Houston, Texas 77030, USA

SUMMARY

Activation of NF-κB, pivotal for immunity and oncogenesis, is tightly controlled by multiple feedback mechanisms. In response to DNA damage, SUMOylation of NEMO (NF-κB essential modulator) is critical for NF-κB activation, however SUMO proteases and feedback mechanisms involved remain unknown. Here we show that among the six known SENPs (Sentrin/SUMO-specific proteases) only SENP2 can efficiently associate with NEMO, deSUMOylate NEMO and inhibit NF-κB activation induced by DNA damage. We further show that NF-κB induces *SENP2* (and *SENP1*) transcription selectively in response to genotoxic stimuli, which involves ATM (ataxia telangiectasia mutated)-dependent histone methylation of *SENP2* promoter κB regions and NF-κB recruitment. SENP2-null cells display biphasic NEMO SUMOylation and activation of IKK and NF-κB, and higher resistance to DNA damage-induced cell death. Our study establishes a self-attenuating feedback mechanism selective to DNA damage induced signaling to limit NF-κB-dependent cell survival responses.

INTRODUCTION

The transcription factor NF-κB is activated by multiple extracellular signals and intracellular stress conditions to control diverse functions, including innate and adaptive immunity and cell death responses (Hayden and Ghosh, 2008; Perkins, 2007). Inactive NF-κB exists in the cytoplasm in association with an inhibitor protein, such as IκBα. Canonical activation of NF-κB requires signaling events that activate IκB kinase (IKK) complexes, composed of catalytic subunits (IKKα/IKK1 and IKKβ/IKK2) and a regulatory subunit IKKγ/NEMO (NF-κB essential modulator). Tight control of NF-κB activity is critical for normal physiology; for example, insufficient activity contributes to the loss of cells in neurodegenerative diseases whereas chronic activity promotes autoimmunity and oncogenesis (Hayden and Ghosh, 2008; Grivennikov et al, 2010; Perkins, 2007).

[5]Correspondence: smiyamot@wisc.edu.

Negative feedback regulation plays an important role in the control of NF-κB activity (Renner and Schmitz, 2009). A classical example is NF-κB-dependent induction of IκBα synthesis following cell stimulation, which directly antagonizes NF-κB (Chiao et al., 1994; Sun et al., 1993). Cells deficient in IκBα show higher basal and more sustained signal-inducible NF-κB activities (Beg et al., 1995). More recent studies have provided examples of feedback regulation acting at or upstream of the IKK activation step. For example, during signaling induced by tumor necrosis factor α (TNFα), receptor interacting protein 1 (RIP1) becomes modified byK63-linked polyubiquitin chains (Liu and Chen, 2011). These ubiquitin chains are thought to function as a signaling scaffold where ubiquitin-binding proteins assemble to induce activation of IKK and NF-κB. Expression of deubiquitinases (DUBs), including A20 and CYLD (cylindromatosis), are also induced by TNFα stimulation in an NF-κB-dependent fashion. These DUBs then remove polyubiquitin chains to limit IKK activation (Brummelkamp et al., 2003; Jono et al., 2004; Kovalenko et al., 2003; Lee et al., 2000; Sun, 2010; Trompouki et al., 2003; Wertz et al., 2004). Consequently, a deficiency in A20 or CYLD can lead to augmented and sustained NF-κB activity in response to inflammatory stimuli and contribute to inflammatory disorders as well as oncogenesis,

Transcriptional regulation of target genes by NF-κB is complex with specificity and temporal regulation driven by κB sites, cell types, specific signals, and others (Hoffmann et al., 2006; Natoli, 2010). In a striking example, one nucleotide substitution in the distal κB element located on the *IP-10* promoter can define signal-specific (TNFα) induction of this gene in a NF-κB family specific manner (p65 dimers) (Leung et al., 2004). Additionally, the chromatin structure is recognized to impose a barrier to NF-κB binding and helps establish the specificity of NF-κB target gene induction. Based on the requirement of prior chromatin modifications, Natoli and colleagues have categorized NF-κB target genes into two broad classes, “fast” and “slow”, where fast genes display constitutive and immediate accessibility of NF-κB association whereas slow genes require a specific chromatin remodeling, such as histone tail methylation, prior to the access of NF-κB to specific κB binding elements (Natoli, 2009).

Among the large number of inducing signals, DNA damage in the nucleus can also trigger activation of NF-κB and represents a unique scenario due to the initiating signal emanating from the nucleus rather than the plasma membrane (Janssens and Tschopp, 2006; Miyamoto, 2011). We previously found that NF-κB activation by genotoxic stimuli involves modification of NEMO by SUMO-1 (small ubiquitin-related modifier 1) (Huang et al., 2003). This SUMOylation seems to occur on IKK-free NEMO and correlates with nuclear localization of NEMO, association with the DNA damage-activated nuclear kinase ATM (ataxia telangiectasia mutated), ATM-dependent phosphorylation (Wu et al., 2006), and subsequent ATM-dependent activation of IKK in the cytoplasm to induce NF-κB activation (Hinz et al., 2010; Wu et al., 2010). Like ubiquitin, SUMO is typically conjugated to lysine residues in target proteins by an E1-E2-E3 enzymatic cascade (Gill, 2004; Hay, 2005; Yeh, 2009). One E1 (an AOS1-UBA2 dimer), one E2 (UBC9) and multiple E3s are known to induce protein SUMOylation (Ulrich, 2005; Yeh, 2009). Our studies have revealed that the E3, PIASy (protein inhibitor of STAT y, also known as PIAS4/PIASγ), mediates SUMOylation of NEMO (Mabb et al., 2006). PIDD (p53-induced death domain protein) and PARP-1 may also participate in the nucleus to promote NEMO SUMOylation (Janssens et al, 2005; Stilmann et al., 2009).

Like DUBs opposing ubiquitination, members of the SENP (Sentrin/SUMO-specific protease) family remove SUMO conjugates (Hay, 2007; Yeh, 2009); however, the potential role of SUMO proteases in regulation of NF-κB signaling remains unknown. It is also unclear whether NF-κB could regulate the expression of SENPs, similar to certain DUBs, to negatively regulate NF-κB signaling. Here we addressed these questions and showed that

SENP2 and SENP1 are major and minor negative regulators, respectively, of NF-κB signaling induced by genotoxic stimuli. We also revealed that the genes encoding these SUMO proteases are direct NF-κB targets selectively induced under DNA damage conditions. Our study reveals a negative feedback mechanism selectively induced by genotoxic stimuli involving NF-κB-dependent induction of SUMO proteases to limit NF-κB-dependent cell survival responses, which may have implications in oncogenesis and cancer progression.

RESULTS

SENP2 Interacts with NEMO and Limits NF-κB Activation by Genotoxic Stimuli

There are six SUMO protease genes (*SENP1, 2, 3, 5, 6* and *7; SENP4* does not exist) known in the human genome (Hay, 2007; Yeh, 2009). To determine if any of these could modulate NF-κB signaling induced by genotoxic signals, we took three independent approaches. First, to reveal which of the SENPs had the potential to interact with NEMO, different SENPs were co-expressed with NEMO in HEK293 cells and their interaction was assessed by co-immunoprecipitation (co-IP) analysis following treatment with the topoisomerase inhibitor etoposide (VP16). Of all the SENPs, SENP2 was the most efficient in interacting with NEMO (Fig. 1A). Second, their impact on NF-κB activation by VP16 was evaluated by electrophoretic mobility shift assay (EMSA) following overexpression of individual *SENPs*. Again, only SENP2 expression significantly inhibited NF-κB activation induced by VP16 (Fig. 1B) with a maximum observable inhibition of ~50% (Fig. 1C), likely due to relatively high basal SENP2 expression in this cell type (see below). In contrast to the wild type (wt) version, overexpression of a catalytically inactive cysteine-to-serine SENP2 mutant (c/s) caused an increase of NF-κB activation (Fig. 1D). Similarly, κB-dependent luciferase reporter assay also showed significant decrease and increase in NF-κB activation upon expression of SENP2-wt and -c/s, respectively (Fig. 1E–F, others not shown). This suggested that the catalytic activity of SENP2 is required to mediate NF-κB inhibition and that the catalytically inactive mutant might function in a dominant-negative manner. Finally, the change in NF-κB activation was analyzed upon expression of siRNAs targeting individual *SENPs*. SENP2 knockdown caused increased NF-κB activation by VP16 (Fig. S1A–C, Fig. 1E–F). Knockdown of SENP7 was also associated with an increase in NF-κB activation by VP16 (Fig. S1A–C) but not by topoisomerase I inhibitor camptothecin (CPT) or doxorubicin (not shown). In contrast, SENP2 showed functional significance with different genotoxic stimuli in multiple cell systems (see below). Thus, three independent experimental approaches suggested SENP2 was the main negative regulator of NF-κB signaling induced by genotoxic agents.

SENP2 DeSUMOylates NEMO

Since SENP2 is primarily localized in the nucleus (Hang and Dasso, 2002) and SUMOylation of NEMO is thought to be a nuclear event (Janssens et al., 2005; Mabb et al., 2006; Stilmann et al., 2009), we next tested whether SENP2 could modulate NEMO SUMOylation. Overexpression of SENP2-wt decreased the amount of SUMOylated NEMO induced by VP16 (Fig. 2A). In contrast, SENP2-c/s mutant caused a slight increase in NEMO SUMOylation, consistent with the observed increase in NF-κB activation (Fig. 1D). Interaction of endogenous SENP2 and NEMO was induced by VP16 treatment (Fig. 2B). NEMO deletion analysis indicated that its N-terminal region is required for SENP2 interaction (Fig. 2C). As predicted, the SENP2-c/s mutant interacted with NEMO (Fig. S2A), which required the central region of SENP2 (Fig. 2D). Finally, SENP2 interacted more efficiently with a SUMO1-NEMO fusion protein than with NEMO alone (Fig. 2E), suggesting that addition of the SUMO-1 moiety increased SENP2 interaction.

We previously showed that the recombinant catalytic domain of SENP1 could deSUMOylate NEMO *in vitro* (Mabb et al., 2006). Similarly, a recombinant SENP2 catalytic domain deSUMOylated NEMO *in vitro* (Fig. S2B). When different amounts of full-length SENP1 and SENP2 were analyzed in parallel in their abilities to deSUMOylate NEMO *in vitro*, SENP2 was found to be more proficient than SENP1 (Fig. 2F), correlating with the ability of SENP2 but not SENP1 to efficiently interact with NEMO (Fig. 1A). Consistent with the idea that SENP2 acts on SUMOylated NEMO upstream of IKK activation, SENP2 expression also reduced IKK activation (Fig. S2C) and IKK-dependent phosphorylation of IκBα (Fig. S2D). We conclude that SENP2 can inhibit NF-κB activation by DNA damage via NEMO deSUMOylation. SENP1 may also induce NEMO deSUMOylation *in vitro* but its *in vivo* effects on NEMO deSUMOylation and NF-κB response induced by DNA damage are much less efficient than those induced by SENP2.

SENP2 and *SENP1* are NF-κB-Inducible Genes

The synthesis of negative regulatory DUBs during cytokine signaling, particularly A20, is induced by NF-κB to attenuate the NF-κB response (Lee et al., 2000; Wertz et al., 2004; Sun, 2010). We therefore tested if *SENP2* expression could be induced by NF-κB in response to DNA damage by analyzing the expression of *SENP2* (and all other *SENP* genes) by qRT-PCR in several cell lines (HEK293, CEM T-cell leukemia, MDA-MB-231 breast carcinoma) treated with genotoxic agents or TNFα. Significantly, *SENP2* was induced by treatment with VP16 in all cell systems analyzed (Fig. 3A–C, others not shown). *SENP1*, but not other *SENPs*, was also induced by VP16 (Fig. 3A–C). The magnitude of the induction varied from 3- to >20-fold depending on the cell type. CPT also induced both *SENP2* and *1* in HEK293 cells (not shown). Significantly, induction of *SENP2* and *1* genes seen in parental cells was not observed in IκBα-S32/36A expressing cell lines (Fig. 3B–C), in which IKK-dependent phosphorylation sites of IκBα were mutated causing inhibition of NF-κB activation and function (Fig. 3D, S3A–B). The increases in *SENP2* mRNA were mirrored by slightly delayed accumulation of SENP2 protein and decreased NF-κB activity in CEM cells with relatively low basal levels of SENP2 protein (Fig. 3E, S3C). Increased SENP2 levels correlated with decreased SUMOylated NEMO and resistance to NF-κB activation in response to a sequential DNA damage challenges induced by CPT and VP16 (Fig. S3D–F). This was not due to alterations in cell cycle status of the CPT-treated cells since NF-κB activation by VP16 is not coupled to specific cell cycle phases (Wuerzberger-Davis et al., 2005). In contrast, TNFα failed to induce *SENP2* and *SENP1* genes in all cell lines analyzed (Fig. 3A, others not shown).

SENP2 and *SENP1* Genes are Direct NF-κB Targets

To determine if the induction of *SENP2* (and *SENP1*) by NF-κB occurs via a direct mechanism, we next scanned the presence of putative κB sites in the *SENP2/1* loci based on JASPAR database analysis and identified multiple putative κB elements in the 5′ regions of both genes (Fig. S4A). To test whether NF-κB directly associated with the *SENP2/1* 5′ regions, chromatin-immunoprecipitation (ChIP) was performed to measure the occupancy of p65 (RelA) and the transcriptional coactivator CBP. Both p65 and CBP bound to the κB-4and -7 regions (κB-7 site had two adjacent sites, termed κB-7.1 and -7.2) located upstream of the *SENP2* start site sequence (Fig. 4A–B) and the κB-6 region (the κB-6 site had two adjacent sites, κB-6.1 andκB-6.2) in the *SENP1* locus (Fig. S4B) in VP16-treated CEM and HEK293 cells (others not shown). In contrast, p65 failed to bind these sites following treatment with TNFα (Fig. 4C). EMSA and supershift analyses using oligonucleotides corresponding to these *SENP2* and *SENP1* κB sites confirmed their association with p65 activated by genotoxic signals (Fig. S4C–D).

To test the functional role of κB sites in the *SENP2* promoter/enhancer, we constructed a luciferase reporter cassette containing a 2.5kb *SENP2* upstream region appended 5′ to the luciferase reporter gene. VP16 exposure of HEK293 cells transfected with this construct caused a robust induction of the luciferase activity (Fig. 4D). While mutation of the κB-4 site caused a modest reduction in reporter activity, mutations of the κB-7.1 and -7.2 sites abrogated induction. These results demonstrated that κB-7 sites were the principal functional NF-κB binding elements for *SENP2* induction in response to DNA damage, correlating with the magnitude of p65 recruitment (Fig. 4B). Interestingly, TNFα exposure that failed to induce p65 recruitment to the endogenous *SENP2* κB sites (Fig. 4B) nevertheless caused strong induction of the *SENP2* 5′-luciferase reporter activity (Fig. 4E). These results demonstrated that the *SENP2* locus imposed DNA damage specificity that was lost when 5′ elements were displaced from their endogenous chromatin context.

ATM-Dependent Histone Methylation of *SENP2* 5′ κB Regions

The above observations suggested the possibility that the *SENP2* gene is a “slow” NF-κB target gene that requires signal-specific chromatin remodeling before NF-κB gains access to κB sequences (Natoli, 2009). During initiation of transcription, methylation of histone H3 lysine 4 (H3K4) increases the access of the transcription machinery (Cedar and Bergman, 2009; Natoli, 2010). Modulation of the transcriptional repressive marks (e.g., H3K9me2, H3K27me3) may also accompany transcriptional activation. We evaluated several histone modifications (H3K4me1, H3K4me2, H3K9me2, H3K27me3) in the *SENP2* 5′ κB regions by ChIP analysis before and after DNA damage stimuli. The amount of H3K4me2 spanning the two critical κB sites in the *SENP2* 5′ sequence (κB-7 and κB-4 sites) was increased after VP16 treatment 20–40-fold when corrected for total H3 levels, but not by TNFα exposure (Fig. 5A, S5A–S5B). Repressive H3K9me2 and H3K27me3 modifications in these regions were nearly undetectable without stimulation and no changes in their status were seen after genotoxic insults (not shown). The increase in the level of H3K4me2 over the κB-7 region was still observed in IκBα-S32/36A expressing HEK293 cells (Fig. 5B). In contrast, the increase in the level of H3K4me2 across κB-4 region was not observed in IκBα-S32/36A expressing HEK293 cells (Fig. 5B), indicating that the histone methylation at the major functional κB-7 region was NF-κB independent but that at the minor κB-4 region was NF-κB dependent. Preincubation with the ATM inhibitor KU55933 (Fig. 5C) or silencing of ATM expression by siRNA (Fig. 5D) eliminated the increase in H3K4me2 at both the κB-7 and κB-4 regions with VP16 treatment, showing that ATM was required to increase modifications at both κB regions. Inhibition of NF-κB by IκBα-S32/36A did not affect ATM expression (Fig. S5C; De Siervi et al., 2009). Thus, NF-κB-dependent induction of *SENP2* involved the ATM-dependent chromatin remodeling of the *SENP2* κB regions.

SENP2 Limits Biphasic NEMO SUMOylation and NF-κB Activation

Since our data thus far indicated that SENP2 was the major SUMO protease for NEMO and an inducible negative regulator of NF-κB activation by DNA damage. SENP2 deficiency should result in higher and more sustained NF-κB activity. Deficiency of SENP1, a possible weak secondary inhibitor of NF-κB, may result in a modest activation. To test these hypotheses, we compared NF-κB activity in wild type (*Wt*), *Senp2*$^{-/-}$ (Kang et al., 2010), and *Senp1*$^{-/-}$; (Cheng et al., 2007) MEF cells. In these analyses, we employed CPT since NF-κB activation by VP16 as measured by EMSA was generally undetectable in these cells (not shown). Activation of NF-κB by CPT exposure in *Wt* cells was induced transiently peaking around 2 h following stimulation (Fig. 6A–B). In *Senp2*$^{-/-}$ cells, basal activity was slightly higher and CPT-induced peak activation was ~3-fold higher at 2 h. Interestingly, CPT induced a second phase of NF-κB activation after 6 h that was not observed in *Wt* cells. Re-expression of the *SENP2* gene in *Senp2*$^{-/-}$ MEFs reduced the peak NF-κB activation observed at 2 h (Fig. S6A). In *Senp1*$^{-/-}$ cells, both basal and CPT-induced peak NF-κB

activation was intermediate between *Wt* and *Senp2*$^{-/-}$ cells. Importantly, similar to *Wt* cells, the second phase of activation was not observed. The lack of the second phase activation in *Wt* cells was associated with increased *Senp2*, but not *Senp1*, induction (Fig. S6B).

We next assessed whether the increased NF-κB activation in *Senp2*$^{-/-}$ MEFs was associated with increased NEMO SUMOylation status. NEMO SUMOylation was transiently induced at 1 h (Fig. 6C–6D), prior to the peak NF-κB activation seen in these cells (Fig. 6A). NEMO SUMOylation remained low thereafter in *Wt* cells. In contrast, in *Senp2*$^{-/-}$ cells, CPT exposure induced biphasic NEMO SUMOylation peaking at 2–3 h, followed by a second peak at 8 h upon prolonged DNA damage stimuli (Fig. 6C–6D), similar to NF-κB activation seen in these cells (Fig. 6A). Forced expression of SENP2 in *Senp2*$^{-/-}$ MEFs markedly reduced our ability to detect NEMO SUMOylation (Fig. S6C) consistent with reduction of NF-κB activation (Fig. S6A). The total SUMO-1 and SUMO-2/3 modification levels were higher in *Senp2*$^{-/-}$ (and *Senp1*$^{-/-}$) cells compared to *Wt* cells (Fig. S6B), similar to observations made with siRNA analyses (Fig. S1D). IKK kinase assay in CPT-treated *Wt* and *Senp2*$^{-/-}$ cells showed the same trend as that observed for NEMO SUMOylation (Fig. 6F). Thus, the main function of NF-κB-dependent *Senp2* induction was to prevent the second phase of NEMO SUMOylation and IKK and NF-κB activation.

Because NF-κB-dependent induction of IκBα is a well-established mechanism to prevent NF-κB activation, we next tested the possibility that the biphasic activation of NF-κB could be uncoupled into separate IκBα- and NEMO SUMOylation-dependent components. To test this, we next analyzed *Nfkbia*$^{-/-}$ MEF cells devoid of IκBα. In these MEFs, the drop in NF-κB DNA binding was not observed following CPT exposure (Fig. 6G) even though IKK activation was still transient like *Wt* cells (Fig. 6H). Together, these results indicated that IκBα ensures the termination of NF-κB activity while the emergence of second wave of NEMO SUMOylation and IKK activation is prevented by SENP2 in response to chronic genotoxic stimuli.

SENP2 Suppresses NF-κB-Dependent Cell Survival Responses

To determine the functional significance of NF-κB-dependent SENP2 induction in response to DNA damage, we examined whether the loss of SENP2, which resulted in biphasic NF-κB activation (Fig. 6A), impacted cell survival under conditions of genotoxic stress. We observed cleavage of caspase-3 and PARP-1, markers of apoptosis, occurred later and less robustly in *Senp2*$^{-/-}$ cells following CPT exposure compared to *Wt* cells (Fig. 7A–B). These results were further confirmed by cell survival assays where *Senp2*$^{-/-}$ cells were more resistant to CPT-induced death than *Wt* cells (Fig. 7C). This resistance in *Senp2*$^{-/-}$ cells was NF-κB mediated, since expression of IκBα-S32/36A mutant (Fig. S7A) sensitized them to *Wt* levels (Fig. 7C). Moreover, expression of SENP2-wt, but not SENP2-c/s, in *Senp2*$^{-/-}$ cells was able to reverse these effects as measured by PARP-1 cleavage (Fig. 7B) and cell survival assays (Fig. 7D). Finally, knockdown of *Senp2* in *Wt* MEF decreased PARP-1 cleavage (Fig. S7B). Thus, SENP2 deficiency caused NF-κB-dependent resistance to DNA damage-induced apoptotic cell death. *Senp2*$^{-/-}$ cells were not intrinsically resistant to apoptosis as cell death induced by TNFα (+cycloheximide), a treatment that activates a membrane-initiated cell death pathway, was similar to *Wt* cells (Fig. S7C). Collectively, our data support the notion that SENP2 is the primary physiologic SUMO protease for NEMO and NF-κB-dependent induction of SENP2 prevents the second phase of NF-κB activation to significantly limit cell survival response to genotoxic stress.

Discussion

In this study, we uncovered SENP2 as the major SUMO protease for NEMO and an inhibitor of NF-κB activation induced by genotoxic agents. We found that among the six

human SENPs, SENP2 interacted most efficiently with NEMO and most robustly inhibited NF-κB activation by DNA damage stimuli. SENP2 overexpression reduced the level of NEMO SUMOylation and NF-κB activation induced by genotoxic stress. While *Wt* MEFs showed transient NF-κB activation, *Senp2*$^{-/-}$ MEFs showed augmented biphasic genotoxic stress-induced NEMO SUMOylation and NF-κB activation. This was associated with increased resistance to cell death induced by genototic stimuli compared to *Wt* MEFs. All of these effects in *Senp2*$^{-/-}$ cells were reversed by SENP2 expression, confirming the specificity of the SENP2 function. Inhibition of NF-κB activation in *Senp2*$^{-/-}$ MEFs by IκBα-S32/36A mutant sensitized them to DNA damage-induced cell death, thus demonstrating that the changes in cell death response was a consequence of NF-κB activation. Although mutagenesis and functional reconstitution experiments indicated that the sites of SUMOylation and subsequent ubiquitination of NEMO following genotoxc insults are likely the same (Huang et al., 2003), our current data suggest that deSUMOylation *per se* is unnecessary for NF-κB activation by DNA damage. The presence of at least two SUMO and ubiquitin modification sites might allow for signal propagation without the need for SUMO deconjugation.

Although substrate selection by SUMO-specific proteases may depend on the identity of SUMO paralogs and subcellular localization, a complete understanding of the mechanisms by which SENPs select specific substrates is still lacking (Hay, 2007; Mukhopadhyay and Dasso, 2007; Yeh, 2009). We previously showed that SENP1 could remove SUMO-1 from NEMO in an *in vitro* deSUMOylation assay (Mabb et al., 2006), however *in vivo*, SENP1 failed to efficiently interact with NEMO and mediate SUMO removal from this substrate. Instead, SENP2 interacted more efficiently with NEMO *in vivo* and also promoted deSUMOylation *in vitro* more efficiently than SENP1 did. A recent proteomic study also detected a NEMO-SENP2 interaction, although the functional significance of this interaction was not described (Fenner et al., 2010). Since our data showed that SENP2-NEMO interactions could occur in the absence of SUMO-1 modification and involved an N-terminal region of NEMO and a central 200–400 amino acid region of SENP2, SENP2 seems to recognize NEMO via a “docking” mechanism, analogous to certain phosphatases recognizing their substrates without the need for a phospho-moiety (Bose et al., 2006; Endicott et al., 1999). However, a SUMO moiety appears to increase the efficiency of NEMO recognition by SENP2 as a SUMO-1-NEMO fusion protein interacted more efficiently with SENP2 than unmodified NEMO. Since SENP2 possesses a SUMO-interacting motif (SIM) adjacent to the C-terminal catalytic domain (Hecker et al., 2006), the interaction between SUMO-1 and SIM might be involved in further increasing the specificity of SUMOylated NEMO recognition by SENP2 *in vivo*.

We also uncovered that *SENP2 and SENP1* genes are direct targets of NF-κB specifically induced by DNA damage. We are unaware of a report that describes direct modulation of the SUMO pathway components by NF-κB. SENP2 and SENP1 are most closely related to each other and constitute a sub-group among the human SUMO-specific proteases (Hay, 2007; Mukhopadhyay and Dasso, 2007; Yeh, 2009). Coincidentally, the main NF-κB-p65 binding sites (κB-7.1 and -7.2 for *SENP2* and κB-6.1 and -6.2 for *SENP1*) were also similarly located in the 5′ regions of these genes. Interestingly, the cytokine TNFα failed to induce *SENP2*/*1* genes despite its ability to robustly activate NF-κB and induce the *SENP2* promoter-luciferase reporter gene when the promoter is taken out of the endogenous chromatin context. ChIP analysis revealed that VP16, but not TNFα caused H3K4me2 modification at the κB-7 region of *SENP2* promoter, a mark associated with transcriptionally active promoters (Barski et al., 2007; Metzger et al., 2010). This methylation was ATM dependent but independent of NF-κB activation. Thus, it appears that DNA damage-activated ATM promoted a chromatin modification of the κB-7 region of the *SENP2* gene by H3K4me2 to potentially permit subsequent NF-κB recruitment for gene transcription.

This would suggest *SENP2* is a "late" NF-κB target gene requiring chromatin remodeling prior to NF-κB recruitment to κB elements (Natoli, 2009). These findings highlight a role for ATM in chromatin remodeling by H3K4me2 modification to promote transcription of specific target genes, though the mechanism remains unclear. A previous study has described a role for ATM on telomere length regulation with the H3K4 methyltransferase SpSet1p in *S. pombe* (Kanoh et al., 2003) and very recent studies indicated the role of ATM in DNA repair via RNF20 phosphorylation and subsequent regulation in histone methylation, including H3K4me2 (Moyal et al., 2011; Nakamura et al, 2011). Thus, additional studies are warranted to define the mechanism behind ATM-mediated H3K4 methylation of *SENP2* κB regions and identify other genes that are regulated by a similar ATM-NF-κB-dependent mechanism.

Based on these findings, we propose the model depicted in Fig. 7E. This model highlights a conceptual parallel between NF-κB-DUB feedback regulation in cytokine signaling and NF-κB-SENP feedback regulation in DNA damage signaling. In the former induced by TNFα, polyubiquitin modification of signaling proteins, including RIP1, is critical for promoting the formation of signaling complexes to mediate IKK activation (Liu and Chen, 2011). DUBs, such as A20 and CYLD, can disassemble ubiquitin chains and reduce IKK activation to limit NF-κB responses. Moreover, the genes encoding these DUBs are transcriptional targets of NF-κB, thereby establishing a feedback control of IKK activity (Jono et al., 2004; Lee et al., 2000). NF-κB-dependent induction of IκBα forms the second feedback loop that directly inhibits NF-κB activity without impacting on IKK activation (Chiao et al., 1994; Renner and Schmitz, 2009; Sun et al., 1993). In the DNA damage signaling, SUMOylation of NEMO is a critical signaling event to mediate IKK and NF-κB activation (Huang et al., 2003; Janssens et al., 2005; Mabb et al., 2006; Stilmann et al., 2009) and the SUMO protease SENP2 deSUMOylates NEMO to inhibit this pathway. Moreover, transcription of *SENP2* is induced by NF-κB in this signaling context and SENP2 feedback suppresses the second wave of IKK activation to attenuate NF-κB-dependent cell survival responses. SENP1 could potentially form a weaker feedback loop since NF-κB can activate *SENP1* transcription in different cell types and activation of NF-κB is slightly augmented in *Senp1*$^{-/-}$ MEFs following genotoxic stimuli. IκBα is also critical to mediate NF-κB inhibition without attenuating IKK activation in response to DNA damage. As in the case with DUBs in the cytokine signaling (Sun, 2010), the relative significance of NF-κB-dependent feedback regulation mediated by SENPs in genotoxic signaling probably depends on cell types and the nature of DNA damage stimuli, as different cell types display varying propensities to induce these SUMO proteases. This mechanism of DNA damage sensitivity induced by NF-κB-dependent induction of SENP2 contrasts with a recently described NF-κB-dependent pro-cell death mechanism in response to excessive amounts of DNA damage involving a second phase of NF-κB activation mediated by autocrine production of TNFα to induce RIP1-FADD-caspase 8-dependent cell death (Biton and Ashkenazi, 2011). Defining how the magnitude of DNA damage in the nucleus is molecularly decoded to drive NF-κB-mediated cell survival or death responses awaits further investigation.

Stress-induced NF-κB activation that in turn induces SENP2/1 synthesis provides a unique temporal mechanism to coordinate the sumoylation-desumoylation cycle in response to genotoxic stress conditions. Is NF-κB signaling the only process that is modulated by the NF-κB-SENP2/1 pathway induced by DNA damage? Recent studies revealed that SUMO proteins, the SUMO conjugating enzyme UBC9, and SUMO ligases PIAS1 and PIAS4 (PIASy) are recruited to the DNA damage site and mediate SUMOylation of key DNA damage response proteins, including BRCA1 and 53BP1 (Galanty et al., 2009; Morris et al., 2009). SUMOylation of BRCA1 and 53BP1 is required for accumulation of ubiquitinated histone H2A and H2AX at the damage sites and is required for efficient DNA repair. Thus, it is plausible that NF-κB-induced SENP2/1 may also regulate other DNA damage response

components, such as BRCA1 and 53BP1 whose deSUMOylation mechanisms are currently undefined. In this manner, NF-κB-dependent SENP2/1 induction could provide a delayed timing mechanism to deSUMOylate multiple proteins at DNA damage sites to help resolve or reset the DNA damage response. As the DNA damage response is critical for genome integrity and susceptibility to cancer (Jackson and Bartek, 2009; Stracker et al., 2009), identification of other SUMO targets that are regulated by this NF-κB-SENP2/1 axis in response to genotoxic agents may shed additional light on the expanding role of NF-κB in promoting oncogenesis and cancer resistance (Grivennikov et al, 2010).

Experimental Procedures

For further details see Supplemental Information.

Cells, antibodies, and reagents

HEK293 cells, those stably expressing Myc-NEMO or HA-IκBα-S32/36A, and *Wt*, *Senp1*$^{-/-}$ and *Senp2*$^{-/-}$ MEF cells were grown at 37°C in DMEM supplemented with 100 units/mlof penicillin, 1 μg/mlof streptomycin, and 10% fetal bovine serum (FBS). MDA-MB-231, CEM, and those stably expressing HA-IκBα-S32/36A were grown at 37°C in RPMI-medium supplemented as above. Antibodies against Myc (9E10), NEMO (FL-419), IKKα/β (H-470), IκBα (C-21), SENP2 (H-300), p65 (C-20), and CBP (A-22) were purchased from Santa Cruz (CA). Antibodies against tubulin, caspase3, and PARP-1 (Calbiochem, CA), SUMO-1 (GMP1) and SUMO-2 (Invitrogen, CA), NEMO (BD pharmingen, CA), Flag M2 (Sigma, MO), HA (Roche), phospho-S32/S36-IκBα (Cell Signaling), and H3, H3K4me, H3K4m2, H3K9me2 and H3K27me3 (Fishers) were also used. VP16 (10 μM), TNFα (10 ng/ml), CPT (10 μM) and KU55933 (10 μM) were used unless otherwise noted.

HEK293 cells were transiently transfected by a standard Ca^{2+} -phosphate method. *Senp2*$^{-/-}$ MEF cells were electroporated with pQCXIP-3Flag-SENP2 or empty vector and were selected with puromycin (4 μg/ml) to generate pools of stable cells. Transient transfection was performed similarly without the selection with puromycin.

Quantitative RT-PCR

Total RNAs were prepared by RNeasy miniprep kit (Qiagen). cDNAs were synthesized by reverse-transcriptase. Quantitative RT-PCR was performed with appropriate primers and analyzed using Bio-Rad iQ5 system. The primers are shown in Supplementary information. All experiments were done in triplicates for three independent times.

ChIP assay

2×10^6 CEM or HEK293 cells were treated with VP16 or TNFα for 3 h. Cells were then processed as previously described (Wu and Miyamoto, 2008). Briefly, one μg of p65, CBP, H3K4me2, or rabbit IgG antibody was used. DNA-protein complexes were eluted in 150 μL of elution buffer (1% SDS, 0.1 M $NaHCO_3$) for 15 min, twice. DNA-protein cross-links were reversed by incubation at 65°C for overnight. Following treatment with proteinase K, DNA was extracted by Qiagen miniprep kit. Primer pairs used to amplify a specific region of *SENP2* and *SENP1* promoters and all others primers used are listed in Supplementary Information. All analyses were done in triplicates in three independent experiments.

Cell viability assay

5×10^3 cells were seeded on a 6-well plate and cultured for 5 days with or without various doses of CPT. After 5 days, cells were washed with PBS and stained with 0.5% crystal violet solution for 20 min. These cells were then washed with water and dried. To analyze

survival rates, methanol was added to each stained well and the resulting dye signals were read on a spectrophotometer (OD_{540}). All experiments were done in duplicate for three independent times.

Supplementary Material

Refer to Web version on PubMed Central for supplementary material.

Acknowledgments

We thank the members of the Miyamoto lab for helpful discussions. We also thank Drs. Elaine Alarid, Emery Bresnick, Avtar Roopra, John Svarin and Wesley Pike for discussions regarding transcriptional regulation and chromatin modifications. This work was supported by NIH R01 CA77474, CA81065, and GM083681 to S.M. We declare no competing financial interests.

References

Barski A, Cuddapah S, Cui K, Roh TY, Schones DE, Wang Z, Wei G, Chepelev I, Zhao K. High-resolution profiling of histone methylations in the human genome. Cell. 2007; 129:823–837. [PubMed: 17512414]

Beg AA, Sha WC, Bronson RT, Baltimore D. Constitutive NF-κB activation, enhanced granulopoiesis, and neonatal lethality in IκBα-deficient mice. Genes Dev. 1995; 9:2736–2746. [PubMed: 7590249]

Biton S, Ashkenazi A. NEMO and RIP1 control cell fate in response to extensive DNA damage via TNF-α feedforward signaling. Cell. 2011; 145:92–103. [PubMed: 21458669]

Bose R, Holbert MA, Pickin KA, Cole PA. Protein tyrosine kinase-substrate interactions. Curr Opin Struct Biol. 2006; 16:668–675. [PubMed: 17085043]

Brummelkamp TR, Nijman SM, Dirac AM, Bernards R. Loss of the cylindromatosis tumour suppressor inhibits apoptosis by activating NF-κB. Nature. 2003; 424:797–801. [PubMed: 12917690]

Cedar H, Bergman Y. Linking DNA methylation and histone modification: patterns and paradigms. Nat Rev Genet. 2009; 10:295–304. [PubMed: 19308066]

Cheng J, Kang X, Zhang S, Yeh ET. SUMO-specific protease 1 is essential for stabilization of HIF1alpha during hypoxia. Cell. 2007; 131:584–595. [PubMed: 17981124]

Chiao PJ, Miyamoto S, Verma IM. Autoregulation of IκBα activity. Proc Natl Acad Sci USA. 1994; 91:28–32. [PubMed: 8278379]

Compagno M, Lim WK, Grunn A, Nandula SV, Brahmachary M, Shen Q, Bertoni F, Ponzoni M, Scandurra M, Califano A, et al. Mutations of multiple genes cause deregulation of NF-κB in diffuse large B-cell lymphoma. Nature. 2009; 459:717–721. [PubMed: 19412164]

De Siervi A, De Luca P, Moiola C, Gueron G, Tongbai R, Chandramouli GV, Haggerty C, Dzekunova I, Petersen D, Kawasaki E, et al. Identification of new Rel/NF-κB regulatory networks by focused genome location analysis. Cell Cycle. 2009; 8:2093–100. [PubMed: 19502793]

Endicott JA, Noble ME, Tucker JA. Cyclin-dependent kinases: inhibition and substrate recognition. Curr Opin Struct Biol. 1999; 9:738–744. [PubMed: 10607671]

Fenner BJ, Scannell M, Prehn JH. Expanding the substantial interactome of NEMO using protein microarrays. PLoS One. 2010; 5:e8799. [PubMed: 20098747]

Galanty Y, Belotserkovskaya R, Coates J, Polo S, Miller KM, Jackson SP. Mammalian SUMO E3-ligases PIAS1 and PIAS4 promote responses to DNA double-strand breaks. Nature. 2009; 462:935–939. [PubMed: 20016603]

Gill G. SUMO and ubiquitin in the nucleus: different functions, similar mechanisms? Genes Dev. 2004; 18:2046–2059. [PubMed: 15342487]

Grivennikov SI, Greten FR, Karin M. Immunity, inflammation, and cancer. Cell. 2010; 140:883–899. [PubMed: 20303878]

Hang J, Dasso M. Association of the human SUMO-1 protease SENP2 with the nuclear pore. J Biol Chem. 2002; 277:19961–19966. [PubMed: 11896061]

Hay RT. SUMO: a history of modification. Mol Cell. 2005; 18:1–12. [PubMed: 15808504]

Hay RT. SUMO-specific proteases: a twist in the tail. Trends Cell Biol. 2007; 17:370–376. [PubMed: 17768054]

Hayden MS, Ghosh S. Shared principles in NF-κB signaling. Cell. 2008; 132:344–362. [PubMed: 18267068]

Hecker CM, Rabiller M, Haglund K, Bayer P, Dikic I. Specification of SUMO1-and SUMO2-interacting motifs. J Biol Chem. 2006; 281:16117–16127. [PubMed: 16524884]

Hinz M, Stilmann M, Arslan SÇ, Khanna KK, Dittmar G, Scheidereit C. A cytoplasmic ATM-TRAF6-cIAP1 module links nuclear DNA damage signaling to ubiquitin-mediated NF-κB activation. Mol Cell. 2010; 40:63–74. [PubMed: 20932475]

Hoffmann A, Natoli G, Ghosh S. Transcriptional regulation via the NF-κB signaling module. Oncogene. 2006; 25:6706–6716. [PubMed: 17072323]

Huang TT, Wuerzberger-Davis SM, Wu ZH, Miyamoto S. Sequential modification of NEMO/IKKγ by SUMO-1 and ubiquitin mediates NF-κB activation by genotoxic stress. Cell. 2003; 115:565–576. [PubMed: 14651848]

Jackson SP, Bartek J. The DNA-damage response in human biology and disease. Nature. 2009; 461:1071–1078. [PubMed: 19847258]

Janssens S, Tschopp J. Signals from within: the DNA-damage-induced NF-κB response. Cell Death Differ. 2006; 13:773–784. [PubMed: 16410802]

Janssens S, Tinel A, Lippens S, Tschopp J. PIDD mediates NF-κB activation in response to DNA damage. Cell. 2005; 123:1079–1092. [PubMed: 16360037]

Jono H, Lim JH, Chen LF, Xu H, Trompouki E, Pan ZK, Mosialos G, Li JD. NF-κB is essential for induction of CYLD, the negative regulator of NF-κB: evidence for a novel inducible autoregulatory feedback pathway. J Biol Chem. 2004; 279:36171–4. [PubMed: 15226292]

Kang X, Qi Y, Zuo Y, Wand Q, Zou Y, Schwartz RJ, Cheng J, Yeh ET. SUMO-specific protease 2 is essential for suppression of polycomb group protein-mediated gene silencing during embryonic development. Mol Cell. 2010; 38:191–201. [PubMed: 20417598]

Kanoh J, Francesconi S, Collura A, Schramke V, Ishikawa F, Baldacci G, Géli V. The fission yeast spSet1p is a histone H3-K4 methyltransferase that functions in telomere maintenance and DNA repair in an ATM kinase Rad3-dependent pathway. J Mol Biol. 2003; 326:1081–94. [PubMed: 12589755]

Kato M, Sanada M, Kato I, Sato Y, Takita J, Takeuchi K, Niwa A, Chen Y, Nakazaki K, Nomoto J, et al. Frequent inactivation of A20 in B-cell lymphomas. Nature. 2009; 459:712–716. [PubMed: 19412163]

Kovalenko A, Chable-Bessia C, Cantarella G, Israel A, Wallach D, Courtois G. The tumour suppressor CYLD negatively regulates NF-κB signalling by deubiquitination. Nature. 2003; 424:801–805. [PubMed: 12917691]

Lee EG, Boone DL, Chai S, Libby SL, Chien M, Lodolce JP, Ma A. Failure to regulate TNF-induced NF-κB and cell death responses in A20-deficient mice. Science. 2000; 289:2350–2354. [PubMed: 11009421]

Lee JS. Functional link between DNA damage responses and transcriptional regulation by ATM in response to a histone deacetylase inhibitor TSA. Cancer Res Treat. 2007; 39:116–124. [PubMed: 19746225]

Leung TH, Hoffmann A, Baltimore D. One nucleotide in a κB site can determine cofactor specificity for NF-κB dimers. Cell. 2004; 118:453–464. [PubMed: 15315758]

Liu S, Chen ZJ. Expanding role of ubiquitination in NF-κB signaling. Cell Res. 2011; 21:6–21. [PubMed: 21135871]

Mabb AM, Wuerzberger-Davis SM, Miyamoto S. PIASy mediates NEMO SUMOylation and NF-κB activation in response to genotoxic stress. Nat Cell Biol. 2006; 8:986–993. [PubMed: 16906147]

Metzger E, Imhof A, Patel D, Kahl P, Hoffmeyer K, Friedrichs N, Muller JM, Greschik H, Kirfel J, Ji S, et al. Phosphorylation of histone H3T6 by PKCbeta(I) controls demethylation at histone H3K4. Nature. 2010; 464:792–796. [PubMed: 20228790]

Miyamoto S. Nuclear initiated NF-κB signaling: NEMO and ATM take center stage. 2011; 21:116–130.

Morris JR, Boutell C, Keppler M, Densham R, Weekes D, Alamshah A, Butler L, Galanty Y, Pangon L, Kiuchi T, et al. The SUMO modification pathway is involved in the BRCA1 response to genotoxic stress. Nature. 2009; 462:886–890. [PubMed: 20016594]

Moyal L, Lerenthal Y, Gana-Weisz M, Mass G, So S, Wang SY, Eppink B, Chung YM, Shalev G, Shema E, et al. Requirement of ATM-dependent monoubiquitylation of histone H2B for timely repair of DNA double-strand breaks. Mol Cell. 2011; 41:529–542. [PubMed: 21362549]

Mukhopadhyay D, Dasso M. Modification in reverse: the SUMO proteases. Trends Biochem Sci. 2007; 32:286–295. [PubMed: 17499995]

Nakamura K, Kato A, Kobayashi J, Yanagihara H, Sakamoto S, Oliveira DV, Shimada M, Tauchi H, Suzuki H, Tashiro S, Zou L, Komatsu K. Regulation of homologous recombination by RNF20-dependent H2B ubiquitination. Mol Cell. 2011; 41:515–528. [PubMed: 21362548]

Natoli G. Maintaining cell identity through global control of genomic organization. Immunity. 2010; 33:12–24. [PubMed: 20643336]

Natoli G. Control of NF-κB-dependent transcriptional responses by chromatin organization. Cold Spring Harb Perspect Biol. 2009; 1:a000224. [PubMed: 20066094]

Perkins ND. Integrating cell-signalling pathways with NF-κB and IKK function. Nat Rev Mol Cell Biol. 2007; 8:49–62. [PubMed: 17183360]

Renner F, Schmitz ML. Autoregulatory feedback loops terminating the NF-κB response. Trends Biochem Sci. 2009; 34:128–135. [PubMed: 19233657]

Stilmann M, Hinz M, Arslan SC, Zimmer A, Schreiber V, Scheidereit C. A nuclear poly(ADP-ribose)-dependent signalosome confers DNA damage-induced IκB kinase activation. Mol Cell. 2009; 36:365–378. [PubMed: 19917246]

Stracker TH, Usui T, Petrini JH. Taking the time to make important decisions: the checkpoint effector kinases Chk1 and Chk2 and the DNA damage response. DNA Repair (Amst). 2009; 8:1047–1054. [PubMed: 19473886]

Sun SC. CYLD: a tumor suppressor deubiquitinase regulating NF-κB activation and diverse biological processes. Cell Death Differ. 2010; 17:25–34. [PubMed: 19373246]

Sun SC, Ganchi PA, Ballard DW, Greene WC. NF-κB controls expression of inhibitor IκBα: evidence for an inducible autoregulatory pathway. Science. 1993; 259:1912–1915. [PubMed: 8096091]

Trompouki E, Hatzivassiliou E, Tsichritzis T, Farmer H, Ashworth A, Mosialos G. CYLD is a deubiquitinating enzyme that negatively regulates NF-κB activation by TNFR family members. Nature. 2003; 424:793–796. [PubMed: 12917689]

Ulrich HD. SUMO modification: wrestling with protein conformation. Curr Biol. 2005; 15:R257–259. [PubMed: 15823527]

Wertz IE, O'Rourke KM, Zhou H, Eby M, Aravind L, Seshagiri S, Wu P, Wiesmann C, Baker R, Boone DL, et al. De-ubiquitination and ubiquitin ligase domains of A20 downregulate NF-κB signalling. Nature. 2004; 430:694–699. [PubMed: 15258597]

Wu ZH, Miyamoto S. Induction of a pro-apoptotic ATM-NF-κB pathway and its repression by ATR in response to replication stress. EMBO J. 2008; 27:1963–1973. [PubMed: 18583959]

Wu ZH, Shi Y, Tibbetts RS, Miyamoto S. Molecular linkage between the kinase ATM and NF-κB signaling in response to genotoxic stimuli. Science. 2006; 311:1141–1146. [PubMed: 16497931]

Wu ZH, Wong ET, Shi Y, Niu J, Chen Z, Miyamoto S, Tergaonkar V. ATM-and NEMO-dependent ELKS ubiquitination coordinates TAK1-mediated IKK activation in response to genotoxic stress. Mol Cell. 2010; 40:75–86. [PubMed: 20932476]

Wuerzberger-Davis SM, Chang PY, Berchtold C, Miyamoto S. Enhanced G2-M arrest by NF-κB-dependent p21waf1/cip1 induction. Mol Cancer Res. 2005; 3:345–353. [PubMed: 15972853]

Yeh ET. SUMOylation and De-SUMOylation: wrestling with life's processes. J Biol Chem. 2009; 284:8223–8227. [PubMed: 19008217]

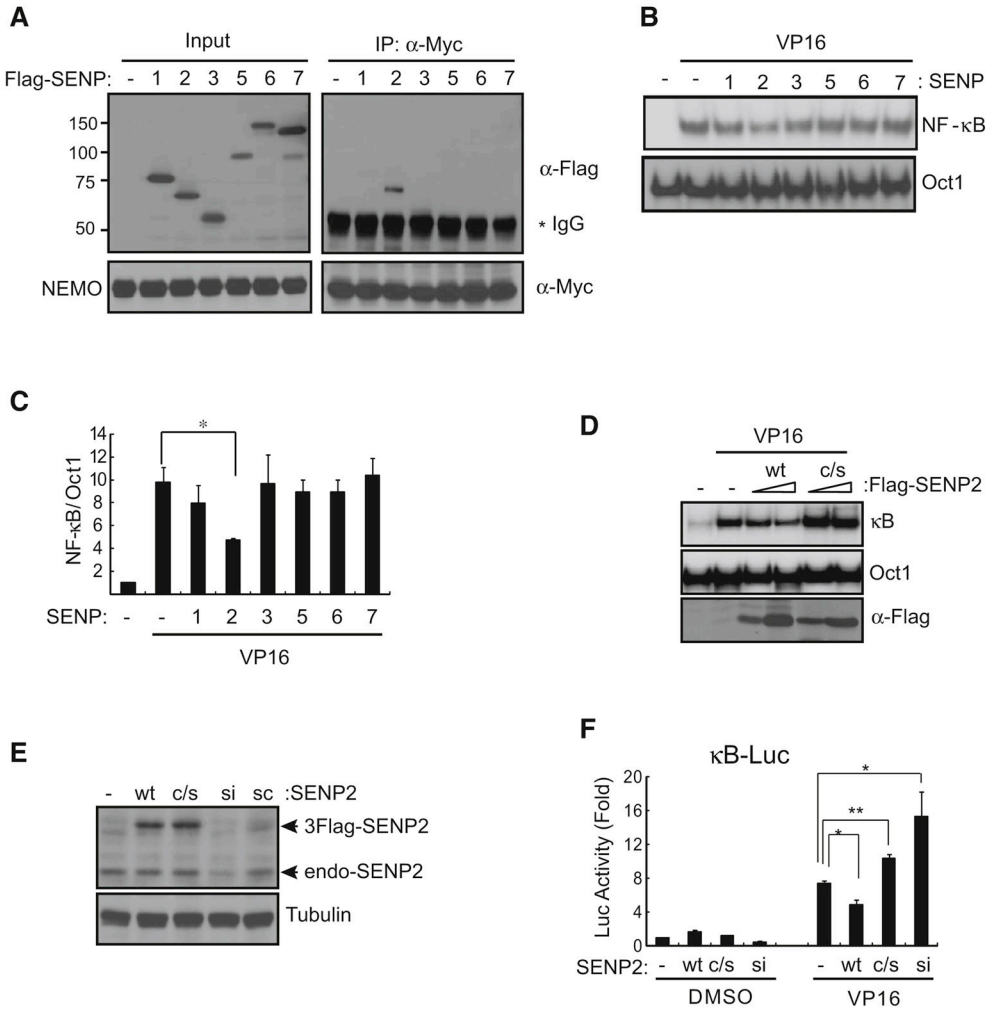

Fig. 1.

SENP2 associates with NEMO and negatively regulates NF-κB activation by genotoxic stress. (A) Flag-SENP1, 2, 3, 5, 6, and 7 were co-transfected with Myc-NEMO in HEK293 cells. Transfected cells were treated with 10 μM VP16 for 1 h, lysed and NEMO was then precipitated with Myc antibody and analyzed by immunoblot using Flag or NEMO antibody. (B) HEK293 cells were transfected with vector (−) or SENP constructs and treated as above. Lysates were used for EMSA using a radio-labeled Igκ-κB or Oct-1 probe. (C) Phosphorimage quantified results from four experiments as in (B) were plotted (mean +SEM). *, $p<0.03$. (D) HEK293 cells were transfected with varying amounts of Flag-SENP2 wild type (wt) or a catalytically inactive mutant (c/s) and were analyzed by EMSA as in (A). (E) HEK293 cells were co-transfected with SENP2-wt, -c/s, or -siRNA (SMARTpool, Dharmacon) and 3x-κB-luciferase and β-galactosidase constructs. Twenty-four hours following transfection, cells were treated with VP16 or DMSO for 8 h and extracts were analyzed by immunoblotting using SENP2 or tubulin antibody. (F) Cell samples as in (E) were analyzed for luciferase and β-galactosidase activities and relative luciferase activity was plotted (mean+SEM). *, $p<0.03$; **, $p<0.001$. See also Figure S1.

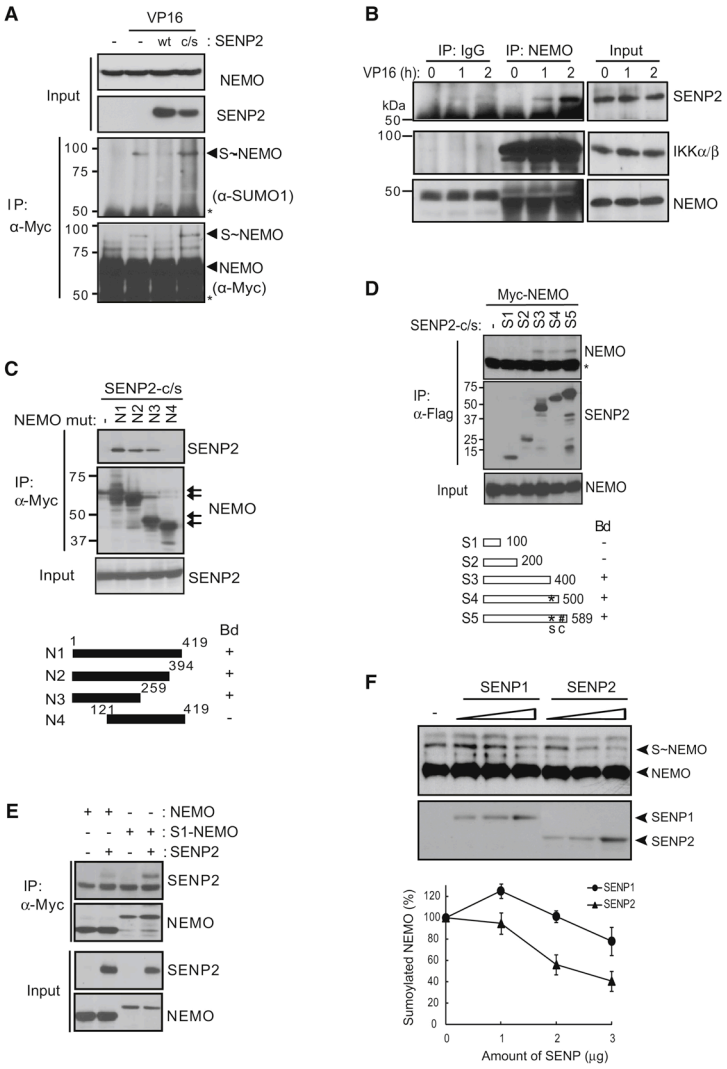

Fig. 2.

SENP2 binds to NEMO and promotes NEMO deSUMOylation. (A) HEK293 cells stably expressing 6xMyc-NEMO were transfected with Flag-SENP2-wt or -c/s constructs, treated with VP16 (1 h) at 24 h after transfection, and then lysed in 1% SDS lysis buffer. Cell lysates were immediately boiled and then SDS diluted to 0.1% final with IP buffer before NEMO was precipitated using Myc antibody for subsequent immunoblot analysis using Myc or SUMO1 antibody. SUMOylated NEMO is indicated by S~NEMO. (*) indicates the IgG heavy chain. (B) HEK293 cells were treated as indicated and used for NEMO IP followed by immunoblot using SENP2, IKKα/β, or NEMO antibody. (C) HEK293 cells were cotransfected with Flag-SENP2-cs and Myc-NEMO truncation constructs (N1–4) and used for Myc IP followed by Flag or Myc immunoblot. Binding data (Bd) data are summarized with diagrams of mutants. (D) HEK293 cells were transfected with Myc-NEMO and Flag-SENP2 truncation constructs (S1–S5) and used for Flag IP followed by Myc or Flag immunoblot. Binding (Bd) data are summarized as above with S (*) indicating SUMO-interaction motif (SIM) and C (#) the catalytic site. (E) HEK293 cells were co-transfected with Myc-NEMO or SUMO-1 (minus the C-terminal di-glycine motif) fused NEMO (S1-NEMO) and Flag-SENP2 and used for Myc IP followed by immunoblotting using indicated antibodies. (F) HEK293 cells were transfected with varying amounts of Flag-SENP1-wt or

Flag-SENP2-wt constructs, treated with VP16 for 1 h and used for Flag IP. SUMOylated NEMO (S~NEMO) was prepared using *in vitro* translation and SUMOylation assay (Mabb et al. 2006). SUMOylated NEMO was incubated with Flag-purified SENP1 or SENP2 for 2 h at 37°C and analyzed by NEMO or Flag immunoblotting. Lower graph: the percentages of SUMOylated NEMO amounts remaining with increasing amounts of transfected SENP constructs are indicated (mean+SD) from two experiments. See also Figure S2.

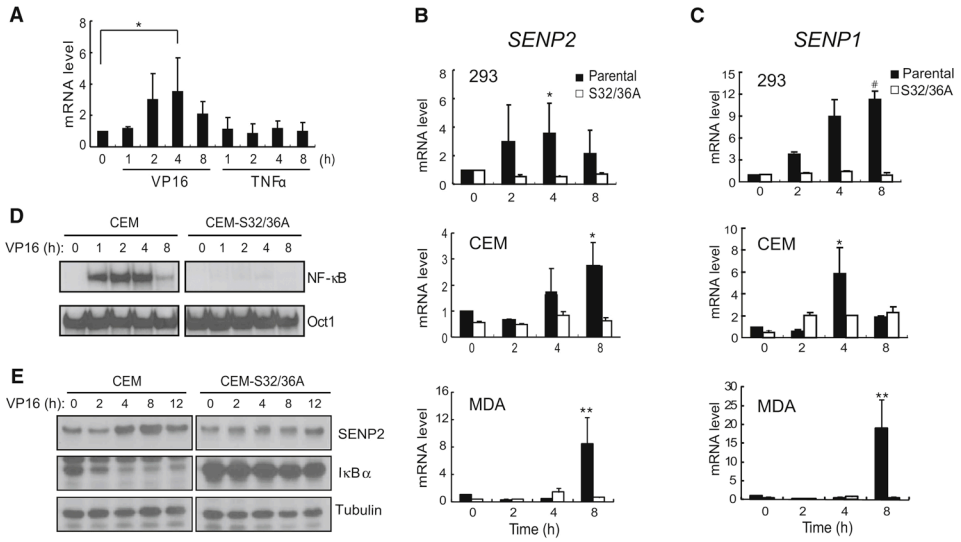

Fig. 3.

SENP2 and *SENP1* genes are NF-κB-regulated genes selectively induced in response to genotoxic stress. (A) HEK293 cells treated as indicated were analyzed for *SENP2* mRNA expression by qRT-PCR and graphed (mean+SEM). (B, C) Indicated parental and those stably expressing HA-IκBα-S32/36A were treated with VP16 for indicated times and analyzed as in (A) for *SENP2* (B) or *SENP1* mRNA (C) expression. The difference compared to untreated samples in parental cells; *, $p<0.05$; **, $p<0.02$; #, $p<0.001$. (D, E) CEM cells and those stably expressing HA-IκBα-S32/36A were treated as indicated and analyzed by EMSA (D) or immunobloting using indicated antibodies (E). See also Figure S3.

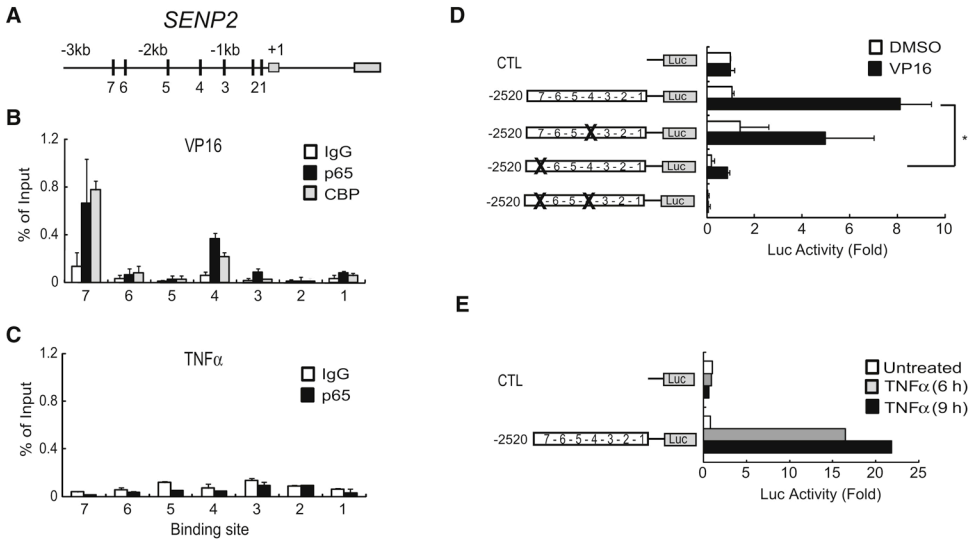

Fig. 4.

SENP2 is a direct NF-κB target gene. (A) A diagram showing putative κB binding sites in the 5′ region of the *SENP2* locus. (B) CEM cells were incubated with VP16 for 3 h and then subjected to ChIP analysis using IgG, p65, or CBP antibodies and qPCR using primers (Supplement Information) spanning each of the putative κB binding sites (indicated with numbers). % input over total qPCR signals for each antibody is shown (mean+SEM). (C) Similar analyses as in (B) were done except for treating cells with TNFα for 3 h. (D) HEK293 cells were transfected with an empty luciferase reporter construct (CTL), *SENP2* 5′ sequence-luc (−2520), or *SENP2* 5′ sequence-luc with the κB sites mutated (indicated by "X"), along with β-galactosidase control vector, and treated with VP16 for 10 h. Luciferase activity corrected for β-galactosidase activity was plotted as fold luciferase activity (mean +SEM). *, $p<0.001$. (E) Similar analyses as in (D) were performed except for exposure of cells to TNFα for times indicated. See also Figure S4.

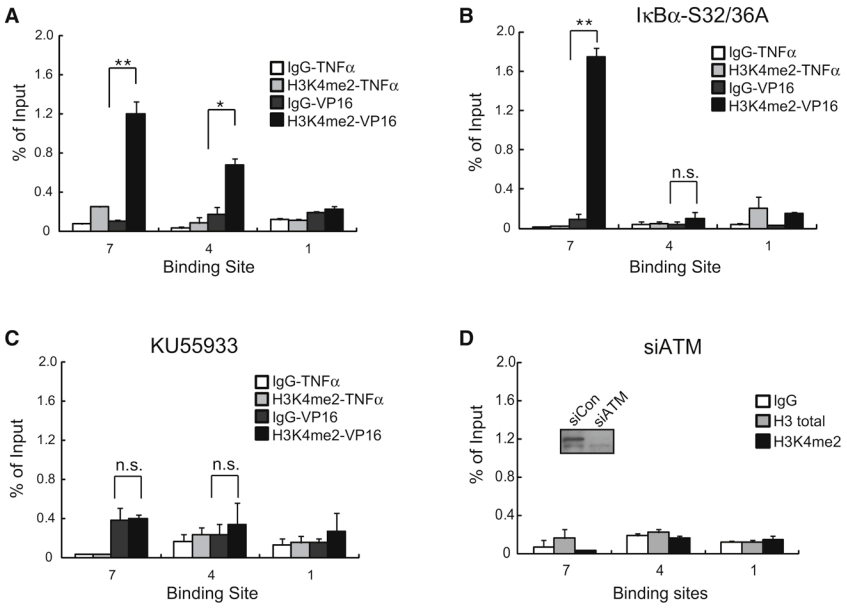

Fig. 5.

ATM-regulated histone methylation of *SENP2* promoter in response to DNA damage. (A) HEK293 cells were incubated with TNFα (T) or VP16 (V) for 3 h. ChIP was performed using H3K4me2 or IgG control antibody and analyzed by qPCR with specific primers around the indicated *SENP2* κB sites. The data are displayed as in Fig. 4B (mean+SEM). *, $p<0.01$. **, $p<0.001$. (B) HEK293 cells stably expressing HA-IκBα-S32/36A were analyzed as in (A). **, $p<0.001$. n.s., not significant. (C) HEK293 cells pretreated with KU55933 for 1 h followed by TNFα (T) or VP16 (V) for 3 h were analyzed as in (A). (D) HEK293 cells were transfected with control or ATM-targeting siRNA and then treated with VP16 (V) for 3 h prior to ChIP analysis using antibodies indicated. The efficiency of ATM knockdown was also evaluated by immunoblotting with ATM antibody. See also Figure S5.

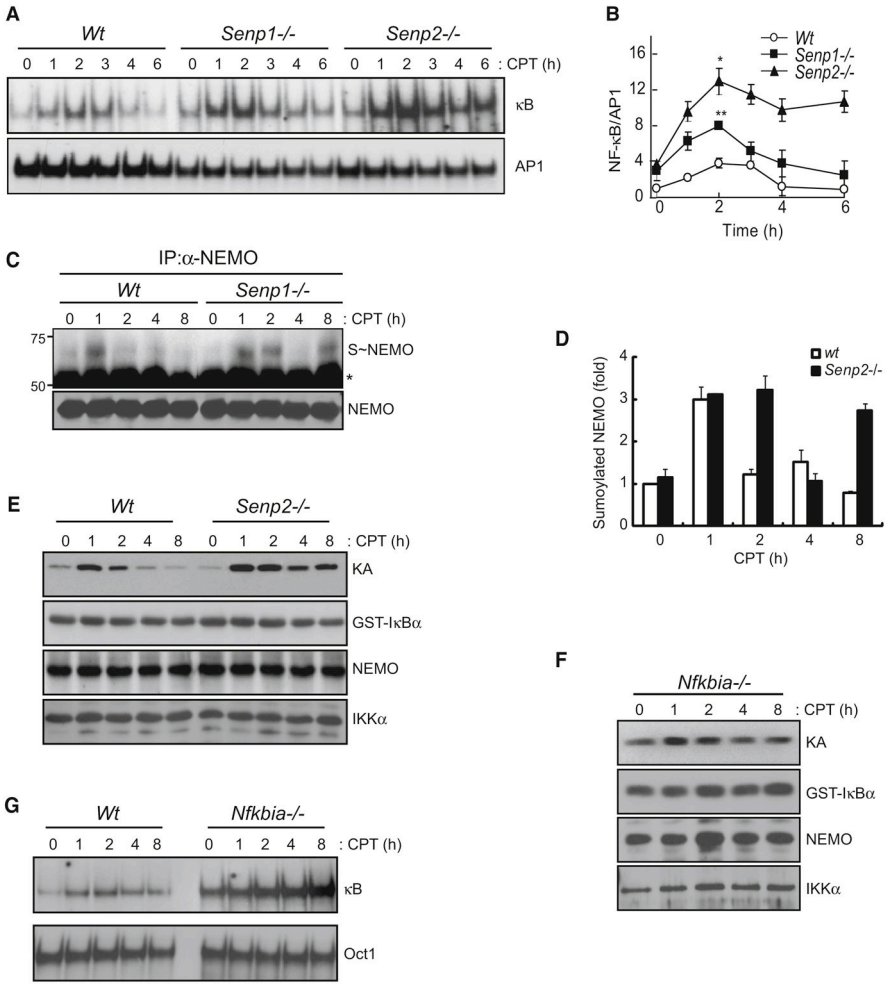

Fig. 6.

SENP2 is required to attenuate a biphasic NEMO SUMOylation and NF-κB activation in response to DNA damage. (A) Different MEFs treated as indicated were analyzed by EMSA. (B) Phosphorimage quantification of NF-κB/AP1 binding from three independent experiments as in (A) was plotted (mean+SD). *p<0.001. **, p<0.01. (C) Different MEFs treated as indicated were processed as in Fig. 2A and SUMOylated NEMO (S~NEMO) was detected by immunoblotting with SUMO1 antibody (upper). (D) S~NEMO signals from (C) from two experiments were quantified by ImageJ analysis of scanned blots and plotted with the mean+SD for each time point indicated. (E) IKK immune-complex kinase assay was performed using GST-IκBα(1–56) as substrate. The amounts of the substrate and NEMO used for IKK immunoprecipitation are shown by immunoblotting. (F) NF-κB activation in *Wt* and *Nfkbia*$^{-/-}$ MEFs were analyzed as in (A). (G) IKK kinase assay was performed using *Nfkbia*$^{-/-}$ MEF as in (E). See also Figure S6.

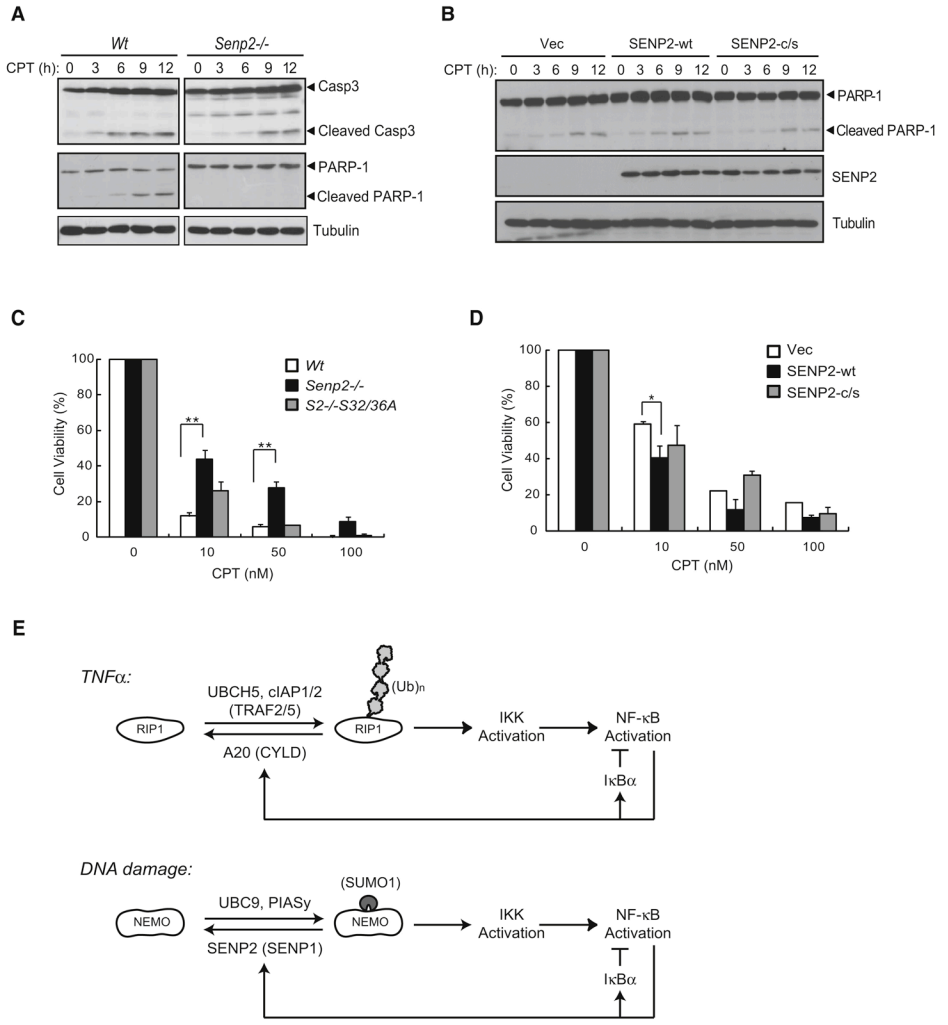

Fig. 7.

SENP2 is required to limit NF-κB-dependent cell survival in response to DNA damage. (A) *Wt* and *Senp2*$^{-/-}$ MEFs treated as indicated were analyzed by immunoblotting with indicated antibodies. (B) *Senp2*$^{-/-}$ MEFs stably reconstituted with SENP2-wt, SENP2-c/s or vector control (Vec) were analyzed as in (A). (C) *Wt*, *Senp2*$^{-/-}$ and *Senp2*$^{-/-}$ stably expressing HA-IκBα-S32/36A (Senp2$^{-/-}$S32/36A) were exposed to different doses of CPT and cell viability was analyzed as in 'Experimental Procedures' and plotted (mean+SEM). (D) MEF cells as in (B) were analyzed as in (C). *, p<0.01. **, p<0.001. (E) A model depicting negative feedback regulation of NF-κB signaling induced by TNFα or DNA damage. See Discussion for details. See also Figure S7.